35th Annual International Conference of the IEEE EMBS
Osaka, Japan, 3 - 7 July, 2013

Accuracy and Uncertainty of Asymmetric Magnetization Transfer Ratio Quantification for Amide Proton Transfer (APT) Imaging at 3T: A Monte Carlo Study

Jing Yuan*, *Senior Member, IEEE*, Qinwei Zhang, *Student Member, IEEE*, Yi-Xiang Wang, Juan Wei, Jinyuan Zhou

Abstract— **Amide proton transfer (APT) imaging offers a novel and powerful MRI contrast mechanism for quantitative molecular imaging based on the principle of chemical exchange saturation transfer (CEST). Asymmetric magnetization transfer ratio (MTR_{asym}) quantification is crucial for Z-spectrum analysis of APT imaging, but is still challenging, particularly at clinical field strength. This paper studies the accuracy and uncertainty in the quantification of MTR_{asym} for APT imaging at 3T, by using high-order polynomial fitting of Z-spectrum through Monte Carlo simulation. Results show that polynomial fitting is a biased estimator that consistently underestimates MTR_{asym}. For a fixed polynomial order, the accuracy of MTR_{asym} is almost constant with regard to signal-to-noise ratio (SNR) while the uncertainty decreases exponentially with SNR. The higher order polynomial fitting increases both the accuracy and the uncertainty of MTR_{asym}. For different APT signal intensity levels, the relative accuracy and the absolute uncertainty keep constant for a fixed polynomial order. These results indicate the limitations and pitfalls of polynomial fitting for MTR_{asym} quantification so better quantification technique for MTR_{asym} estimation is warranted.**

I. INTRODUCTION

Chemical exchange (CE) between free water and biological macro-molecules containing exchangeable labile protons has been recently exploited as a sensitive magnetic resonance imaging (MRI) contrast enhancement mechanism. Chemical exchange MR imaging can be performed by chemical exchange saturation transfer (CEST) imaging [1, 2], T1rho spin-lock imaging [3] or the combined version of chemical exchange spin-lock (CESL) imaging [4, 5]. In CE-MRI, a long saturation radio frequency (RF) pulse is applied at different irradiation offset frequencies and the MR signals are acquired. Z-spectrum is referred as the plot of the signal intensity ratios compared to the unsaturated signal intensity as a function of offset frequency ($\Delta\Omega$) from water resonance. To eliminate direct water saturation (DS) effect and conventionall magnetization transfer (MT), asymmetric magnetization transfer ratio (MTR_{asym}) is calculated from Z-spectrum. Voxel-wise map of MTR_{asym} provides a heuristic but powerful means of CE-based contrast visualization so as for tissue characterization and lesion detection. In particular, the MTR_{asym} at around 3.5ppm of Z-spectrum visualizes the amide proton transfer (APT) effect and this APT contrast has been shown promising for non-invasive molecular MR imaging with high sensitivity for various pre-clinical and clinical applications [6-10]. The accurate and precise quantification of MTR_{asym} is still challenging. Despite the intrinsic low level of CE contrast particularly at low MRI field strength B0, DS effect cannot be completely eliminated and conventional MT may not be symmetric. Errors arise also from the heterogeneities of tissues and B0/B1 field inhomogeneity. Full Bloch equation fitting of Z-spectrum is extremely difficult due to the complicated dependence of Z-spectrum on many parameters. Therefore, Z-spectrum curve fitting without applying *a priori* model is usually applied in practice, such as the most widely used high-order polynomial fitting and the recently proposed smoothing-spline fitting [11]. In this study, we aim to quantitatively evaluate the accuracy and uncertainty of MTR_{asym} by using polynomial fitting with different orders at different SNRs for APT imaging at 3T through Monte Carlo simulation. This work will be helpful for the optimization of APT imaging protocol and Z-spectrum analysis, as well as the clinical interpretation of MTR_{asym}.

Research supported by Hong Kong GRC grant SEG_CUHK02, CUHK418811, China NSFC grant 81201076 and USA NIH grants R01EB009731, R01CA166171.

J. Yuan* (corresponding author), Q. Zhang and Y-X Wang are with the Department of Imaging and Interventional Radiology, The Chinese University of Hong Kong, Shatin, NT, Hong Kong, China (phone: 852-2632-1036; fax: 852-2636-0012; e-mail: jyuan@cuhk.edu.hk). J. Yuan is also with the CUHK Shenzhen Research Institute, Guangdong, China.

J. Wei is with the Philips research China, Shanghai, China.

J. Zhou is with the Department of Radiology, Johns Hopkins University School of Medicine, Baltimore, Maryland, USA. and F.M. Kirby Research Center for Functional Brain Imaging, Kennedy Krieger Institute, Baltimore, Maryland, USA.

II. METHODS

A. Theoretical model and generation of APT Z-spectrum

Theoretical Z-spectra without any noise were generated according to an asymmetric population two-pool (pool a: water; pool b: amide proton at 3.5ppm offset, i.e. ~448Hz offset at 3T) R1rho relaxation model [12] based on Bloch-McConnell equations [13]. Z-spectrum could be analytically calculated by [4]:

$$\frac{M(\Delta\Omega)}{M_0} = \left(1-\frac{R_1\cdot\cos\theta}{R_{1\rho}}\right)\cdot e^{-R_{1\rho}\cdot T_{sat}} + \frac{R_1\cdot\cos\theta}{R_{1\rho}} \quad (1)$$
$$= \left(1-\frac{R_1\cdot\cos\theta}{R_1\cos^2\theta+(R_2+R_{ex})\sin^2\theta}\right)\cdot e^{-(R_1\cos^2\theta+(R_2+R_{ex})\sin^2\theta)\cdot T_{sat}}$$
$$+\frac{R_1\cdot\cos\theta}{R_1\cos^2\theta+(R_2+R_{ex})\sin^2\theta}$$

where $M(\Delta\Omega)$ and M_0 denote the signal intensity obtained with the saturation RF pulse with the duration of T_{sat} and strength B1 at offset $\Delta\Omega$ and without saturation pulse. θ is calculated as $arctan(2\pi\gamma B1/\Delta\Omega)$. R_{ex} is a complicated term that reflects the relaxation variation due to chemical exchange, dependent on each pool population ($p_a>>p_b$, $p_a+p_b=1$) and resonant frequency, proton exchange rate k and saturation pulse B1 strength. The detail of this modeling could be found in the literatures [4, 5, 12, 14]. R_1 and R_2 are the population averaged tissue spin-lattice relaxation rate and spin-spin relaxation rate, the reciprocal of spin-lattice relaxation time T_1 and spin-spin relaxation time T_2, respectively. MTR_{asym} could be calculated by:

$$MTR_{asym}(\Delta\Omega) = \frac{M(-\Delta\Omega)}{M_0} - \frac{M(\Delta\Omega)}{M_0} \quad (2)$$

Major parameters were set as follows: B_0=3T, $\Delta\Omega_a$=0, $\Delta\Omega_b$=3.5ppm, k=20/s, T_1=1100ms and T_2=69ms (typical values for white matter at 3T) [15]. To simulate different intensities of APT MTR_{asym}, p_b varied from 0.001 to 0.01. The B1 strength and duration of the saturation RF pulse was set as 2μT and 1500ms. Z-spectrum data were obtained using an optimized acquisition protocol [16] at the offsets of [±7, ±6, ±5.5, ±5, ±4.5, ±4, ±3.75, ±3.5, ±3.25, ±3, ±2.5, ±2, ±1.5, ±1, ±0.75, ±0.5, ±0.25, 0] ppm, with higher sampling density around APT offset of 3.5ppm and water resonance. The true APT MTR_{asym} was calculated at ΔΩ=3.5ppm using Eq. 2.

B. Monte Carlo simulation and data analysis

After ideal Z-spectra were generated, Rician noise [17] was imposed on each data point according to the image SNR to produce the noisy Z-spectra. SNR was defined as M_0/σ, where σ was the standard deviation (STD) of noise distribution. Then the noisy Z-spectra were least-square fitted by high-order polynomial-fitting. After fitting, Z-spectra were interpolated to a finer resolution of 0.01ppm. The actual water resonance was assumed to be at the frequency with the lowest intensity of the interpolated Z-spectrum. The original Z-spectra were shifted correspondingly along the offset axis to correct the possible B0 inhomogeneity [7]. Finally, the APT MTR_{asym} was calculated using Eq. 2 at ΔΩ=3.5ppm. This procedure repeated 50,000 times for each combination of polynomial order n, SNR and p_b. Each MTR_{asym} was recorded for statistical analysis purpose.

III. RESULTS AND DISCUSSION

For every combination of polynomial order n, SNR and p_b, the calculated MTR_{asym} (50,000 times) all showed Gaussian distribution. Hence, the accuracy and uncertainty of APT MTR_{asym} could be evaluated respectively by the mean and the STD of the calculated MTR_{asym}.

Figure 1 illustrated two examples of noiseless ideal Z-spectrum, Rician-noise imposed data points at different offset frequencies, least-squared polynomial (n=12) fitted Z-spectrum as well as the true and calculated MTR_{asym} curves at two different SNRs of 20 (a) and 100 (b) when p_b=0.01. The true APT MTR_{asym} at 3.5ppm obtained from the noiseless Z-spectrum was 0.0856, i.e. 8.56% of the unsaturated intensity M_0. Due to the relatively low SNR in Fig.1a, the polynomial fitted Z-spectrum deviated much from the noiseless ideal Z-spectrum and hence led to the error in MTR_{asym} estimation. Even at a very high SNR of 100 (Fig.1b), although the noisy Z-spectrum approaches the ideal one very much, the deviation of the calculated MTR_{asym} from the true values was still noticeable.

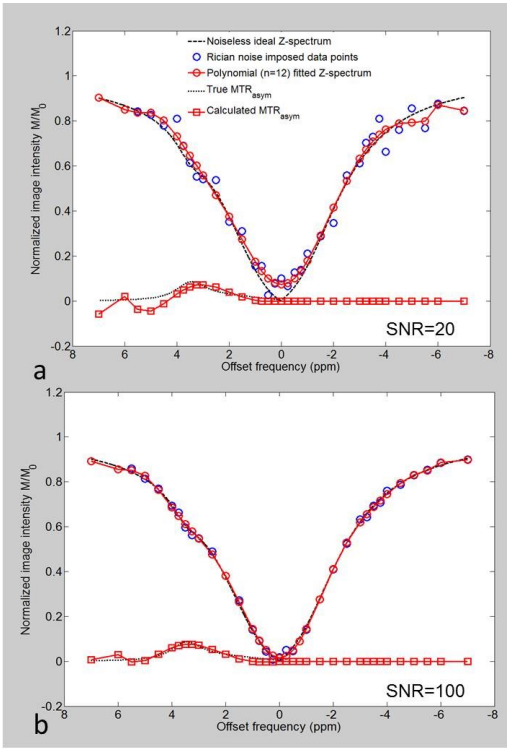

Fig. 1. Illustration of the noiseless ideal Z-spectrum, Rician-noise imposed data points at different offset frequencies, least-squared polynomial (n=12) fitted Z-spectrum as well as the true and calculated MTRasym curves at two different SNRs of 20 (a) and 100 (b) when p_b=0.01.

Figure 2 shows the accuracy (a) and uncertainty (b) of the calculated APT MTR_{asym} by using polynomial fitting with different orders through Monte Carlo simulation. For each polynomial order n, the mean of the calculated APT MTR_{asym} was almost constant (except at very low SNR<20), regardless of SNR. In other words, the accuracy of the calculated MTR_{asym} was independent of SNR for polynomial fitting with a fixed order. Although the polynomial fitting with higher order n remarkably increased the quantification accuracy, more approaching the true MTR_{asym}, all polynomial fitting showed biased under-estimation of MTR_{asym}. As seen from Fig.2b, for each polynomial order n, the uncertainty of MTR_{asym} decreased exponentially with the increasing SNR, which indicated the precision of MTR_{asym} quantification greatly improved from the higher SNR. On the other hand, higher-order polynomial fitting exhibited increased uncertainty although they showed better estimation accuracy compared to the low-order fitting.

The dependence of accuracy and uncertainty of MTR_{asym} quantification on the polynomial order n at a fixed SNR of 80 was shown in Fig 3. Consistent with Fig 2, the accuracy and uncertainty of MTR_{asym} both generally increased with the higher polynomial order n. In addition, it was found that the mean MTR_{asym} approached the true MTR_{asym} asymptotically

with the increasing polynomial order. This indicated that very high order (n>25) polynomial fitting could provide unbiased estimation of MTR_{asym}. However, this unbiasedness of MTR_{asym} estimation was associated with the greatly increased estimation uncertainty. It was also interesting to find that the accuracy and uncertainty did not increase smoothly with polynomial order. For example, the accuracy of MTR_{asym} increased abruptly from n=8 to n=9. The accuracy of MTR_{asym} was almost constant for n=9-12 but increased remarkably when n=13.

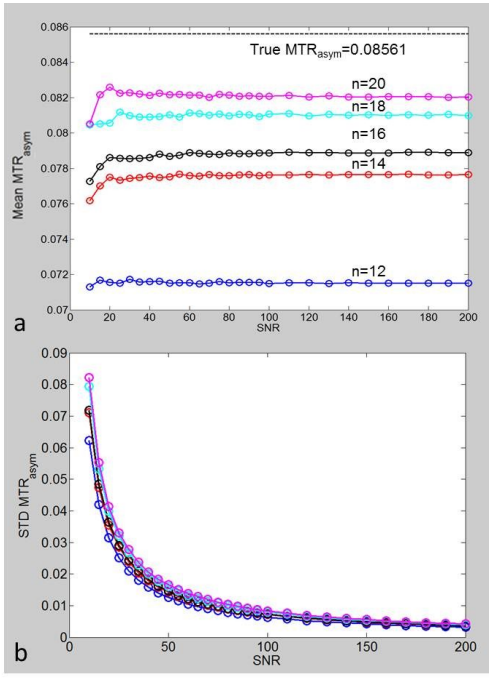

Fig. 2.Monte Carlo simulation result of the accuracy (a) and uncertainty (b) of the calculated APT MTR_{asym} by using polynomial fitting. p_b=0.01.

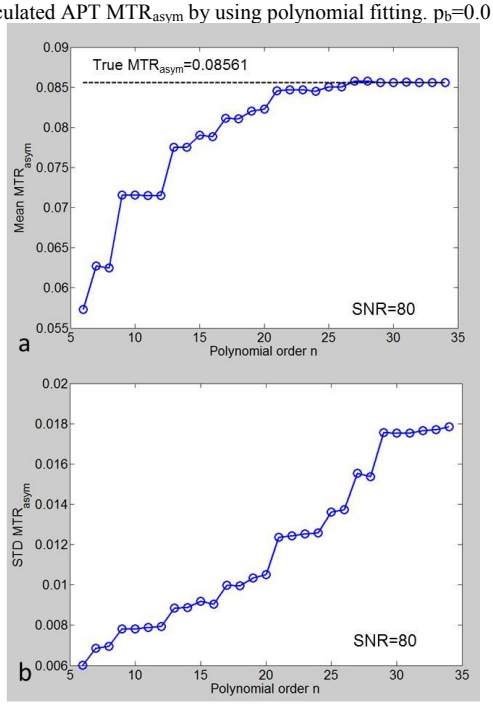

Fig. 3. Dependence of accuracy and uncertainty of MTR_{asym} quantification on the polynomial order n. SNR=80 and p_b=0.01.

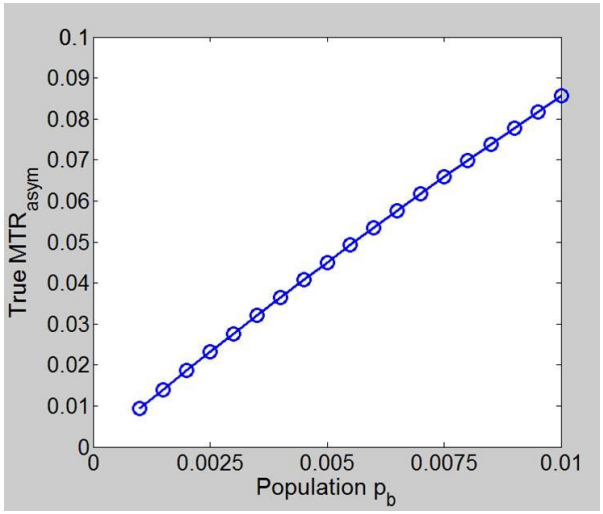

Fig. 4. The linear relationship between pool b population p_b and true MTR_{asym}.

Figure 4 shows the relationship between the population of pool b (p_b) and the true APT MTR_{asym}. It is found that true APT MTR_{asym} increases linearly with p_b, consistent with the theoretical [18] and experiment results [5] for low chemical exchange rate k in the literature.

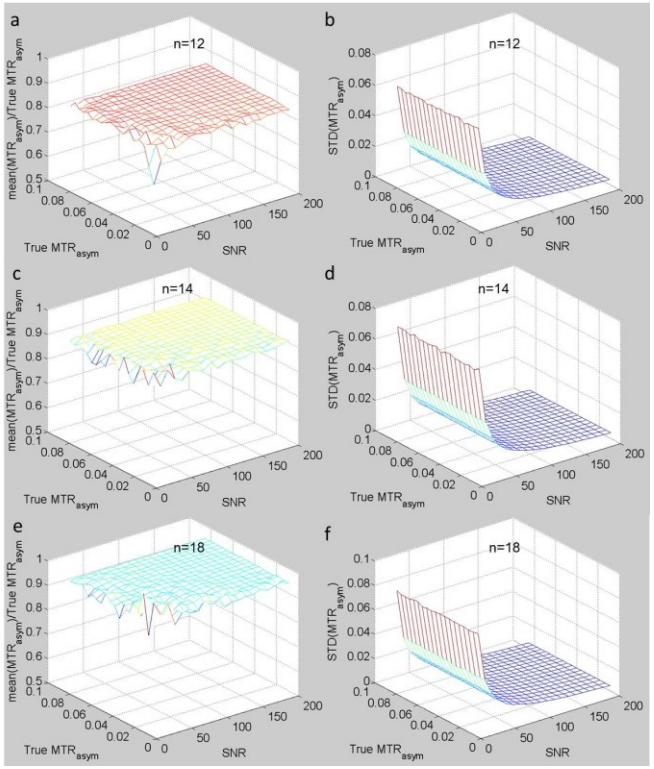

Fig. 5. The dependence of relative accuracy (left column) and absolute standard deviation of MTR_{asym} (right column) on SNR and different true APT MTR_{asym} intensities for polynomial order n=12, 14 and 18.

For different APT signal intensity levels, the dependences of the accuracy (left column) and the uncertainty of the calculated MTR_{asym} (right column) subject to different SNRs are plotted in Fig. 5. Note that the relative accuracy, which was defined as the mean of the calculated MTR_{asym} divided by

the corresponding true MTR_{asym} at a certain SNR, was plotted in Fig. 5 rather than the absolute accuracy shown in Fig. 2-3. As shown in Fig. 5, the relative accuracy generally did not vary with regard to SNR as well as the true MTR_{asym}. Meanwhile, the absolute uncertainty evaluated by the standard deviation of the calculated MTR_{asym}, although exponential decayed with SNR, was not dependent on the true APT MTR_{asym} and remained constant. This finding indicated the increasing difficulty in achieving high precision of MTR_{asym} quantification for lower APT signals since the ratio of the absolute uncertainty and true MTR_{asym} became larger.

This simulation study examined the numerical performance of high-order polynomial fitting for MTR_{asym} quantification in APT imaging. The results indicated the limitations and pitfalls of high-order polynomial fitting for MTR_{asym} quantification. The increased SNR, which is usually associated with the longer scan time, only reduces uncertainty but not improve accuracy. In addition, high-order polynomial fitting is biased and underestimates MTR_{asym} unless very high polynomial order is used, which however inevitably deteriorates the uncertainty. Due to these limitations, the MTR_{asym} calculated by using polynomial fitting in practice, particularly at low SNRs, should be very carefully interpreted.

This study has some limitations. It only includes simulation and experimental verification should be conducted in the future. This study only handles with Rician noise that is only valid for single-coil acquisition. Under multi-coil acquisition, parallel imaging and various image filters, the altered noise characteristics may potentially affect the polynomial fitting results. Currently, Z-spectrum and MTR_{asym} is usually analyzed and quantified by non-parametric regression approaches because the underlying physical model is so complicated. Spline [11] and radial-basis-function networks [19] may be useful alternatives to polynomial fitting, which will be investigated in future studies.

IV. Conclusion

Several conclusions could be drawn from this study. Polynomial fitting is a biased estimator that consistently underestimates MTR_{asym} unless the polynomial order is sufficiently high. For a fixed polynomial order and APT signal intensity, the accuracy of MTR_{asym} is almost constant with SNR while the uncertainty decreases exponentially with SNR. The higher order polynomial fitting increases both the accuracy and the uncertainty of MTR_{asym}. For different APT signal intensity levels, the relative accuracy and the absolute uncertainty keep constant for a fixed polynomial order fitting. Due to these numerical limitations and pitfalls, MTR_{asym} quantified by using high-order polynomial fitting in practice should be carefully interpreted. Better estimators are warranted in the future studies to improve accuracy and precision of MTR_{asym} quantification.

References

[1] P. C. van Zijl and N. N. Yadav, "Chemical exchange saturation transfer (CEST): what is in a name and what isn't?," *Magn Reson Med,* vol. 65, pp. 927-48, Apr 2011.

[2] K. M. Ward, A. H. Aletras, and R. S. Balaban, "A new class of contrast agents for MRI based on proton chemical exchange dependent saturation transfer (CEST)," *J Magn Reson,* vol. 143, pp. 79-87, Mar 2000.

[3] Y. X. Wang, J. Yuan, E. S. Chu, M. Y. Go, H. Huang, A. T. Ahuja*, et al.*, "T1rho MR Imaging Is Sensitive to Evaluate Liver Fibrosis: An Experimental Study in a Rat Biliary Duct Ligation Model," *Radiology,* vol. 259, pp. 712-9, Jun 2011.

[4] J. Yuan, J. Zhou, A. T. Ahuja, and Y. X. Wang, "MR chemical exchange imaging with spin-lock technique (CESL): a theoretical analysis of the Z-spectrum using a two-pool R(1rho) relaxation model beyond the fast-exchange limit," *Phys Med Biol,* vol. 57, pp. 8185-8200, Nov 23 2012.

[5] T. Jin, J. Autio, T. Obata, and S. G. Kim, "Spin-locking versus chemical exchange saturation transfer MRI for investigating chemical exchange process between water and labile metabolite protons," *Magn Reson Med,* vol. 65, pp. 1448-60, May 2011.

[6] J. Y. Zhou, J. F. Payen, D. A. Wilson, R. J. Traystman, and P. C. M. van Zijl, "Using the amide proton signals of intracellular proteins and peptides to detect pH effects in MRI," *Nature Medicine,* vol. 9, pp. 1085-1090, Aug 2003.

[7] J. Zhou, B. Lal, D. A. Wilson, J. Laterra, and P. C. van Zijl, "Amide proton transfer (APT) contrast for imaging of brain tumors," *Magn Reson Med,* vol. 50, pp. 1120-6, Dec 2003.

[8] C. K. Jones, M. J. Schlosser, P. C. van Zijl, M. G. Pomper, X. Golay, and J. Zhou, "Amide proton transfer imaging of human brain tumors at 3T," *Magn Reson Med,* vol. 56, pp. 585-92, Sep 2006.

[9] A. N. Dula, L. R. Arlinghaus, R. D. Dortch, B. E. Dewey, J. G. Whisenant, G. D. Ayers*, et al.*, "Amide proton transfer imaging of the breast at 3 T: Establishing reproducibility and possible feasibility assessing chemotherapy response," *Magn Reson Med,* Aug 20 2012.

[10] G. Jia, R. Abaza, J. D. Williams, D. L. Zynger, J. Zhou, Z. K. Shah*, et al.*, "Amide proton transfer MR imaging of prostate cancer: a preliminary study," *J Magn Reson Imaging,* vol. 33, pp. 647-54, Mar 2011.

[11] J. Stancanello, E. Terreno, D. D. Castelli, C. Cabella, F. Uggeri, and S. Aime, "Development and validation of a smoothing-splines-based correction method for improving the analysis of CEST-MR images," *Contrast Media Mol Imaging,* vol. 3, pp. 136-49, Jul-Aug 2008.

[12] O. Trott and A. G. Palmer, 3rd, "R1rho relaxation outside of the fast-exchange limit," *J Magn Reson,* vol. 154, pp. 157-60, Jan 2002.

[13] H. M. McConnell, "Reaction rates by nuclear magnetic resonance," *J Chem Phys,* vol. 28, pp. 430-1, 1958.

[14] T. Jin, P. Wang, X. Zong, and S. G. Kim, "Magnetic resonance imaging of the Amine-Proton EXchange (APEX) dependent contrast," *Neuroimage,* vol. 59, pp. 1218-27, Jan 16 2012.

[15] G. J. Stanisz, E. E. Odrobina, J. Pun, M. Escaravage, S. J. Graham, M. J. Bronskill*, et al.*, "T1, T2 relaxation and magnetization transfer in tissue at 3T," *Magn Reson Med,* vol. 54, pp. 507-12, Sep 2005.

[16] J. Zhou, J. O. Blakeley, J. Hua, M. Kim, J. Laterra, M. G. Pomper*, et al.*, "Practical data acquisition method for human brain tumor amide proton transfer (APT) imaging," *Magn Reson Med,* vol. 60, pp. 842-9, Oct 2008.

[17] H. Gudbjartsson and S. Patz, "The Rician distribution of noisy MRI data," *Magn Reson Med,* vol. 34, pp. 910-4, Dec 1995.

[18] P. Z. Sun, "Simultaneous determination of labile proton concentration and exchange rate utilizing optimal RF power: Radio frequency power (RFP) dependence of chemical exchange saturation transfer (CEST) MRI," *J Magn Reson,* vol. 202, pp. 155-61, Feb 2010.

[19] S. Chen, C. F. N. Cowan, and P. M. Grant, "Orthogonal Least-Squares Learning Algorithm for Radial Basis Function Networks," *Ieee Transactions on Neural Networks,* vol. 2, pp. 302-309, Mar 1991.